

# Microporous Silica Hollow Microspheres and Hollow Worm-Like Materials: A Simple Method for Their Synthesis and Their Application in Controlled Release

Mingwei Zhao,<sup>[a]</sup> Yanan Gao,<sup>[a]</sup> Liqiang Zheng,<sup>\*[a]</sup> Wenpei Kang,<sup>[a]</sup> Xiangtao Bai,<sup>[a]</sup> and Bin Dong<sup>[a]</sup>

**Keywords:** Microporous materials / Nanostructures / Template synthesis / Evaporation method / Ionic liquids

Hollow silica microspheres and hollow worm-like materials were synthesized by using a simple method with the aid of 1-dodecyl-3-methylimidazolium bromide (C<sub>12</sub>mimBr). Hollow silica microspheres were initially produced by utilizing the combination of evaporation and an emulsion template. At a longer mixing time, the microspheres fused to form hollow worm-like silica materials due to the fusion of the emulsion templates. The resultant silica materials were characterized by transmission electron microscopy (TEM), scanning elec-

tron microscopy (SEM), and nitrogen adsorption/desorption. Both the hollow silica microspheres and the hollow worm-like materials are microporous. On the basis of experimental observations and the resulting products, a plausible formation mechanism is proposed. Preliminary tests demonstrate that the hollow silica microspheres and worm-like materials are capable of being loaded with Rhodamine B and releasing it, thus showing a great potential in controlled delivery applications.

## 1. Introduction

Because the properties of materials with the same composition but different morphologies can be substantially different, scientists have paid more attention to the design of materials with controlled size, physical characteristics, and morphology. Some examples are hollow materials,<sup>[1]</sup> nanoparticles,<sup>[2]</sup> nanowires,<sup>[3]</sup> nanotubes,<sup>[4]</sup> and many other unique structures.<sup>[5–7]</sup> Of the variety of forms described in the literature, the controlled synthesis of hollow micro- or nanomaterials have drawn much interest because of their potential applications in areas such as controlled drug delivery, catalysis, chemo- and biosensors, photonic crystals, and biomedical diagnosis and therapy.<sup>[8–12]</sup> Due to their special properties, including high surface area, low density, large fractional void space, and so on, many synthesis methods for hollow materials have been developed, which may be generally separated into those using a template and template-free ones. Both approaches are convenient and have been widely used to fabricate hollow materials promoting the recent development of this area of nanoscience and surfactant self-assembly.

The synthesis of hollow materials without templates is usually very simple and mainly involves evaporation,<sup>[13]</sup> spray drying,<sup>[14]</sup> ultrasonication,<sup>[15]</sup> laser pyrolysis,<sup>[16]</sup> or

other methods. Among these template-free methods, the evaporation method appears to be generally effective in the synthesis of hollow materials.<sup>[17–20]</sup> Baskaran et al. initially reported the synthesis of mesostructured silica fibers and hollow spheres with this method.<sup>[17]</sup> Mesoporous fibers were prepared by dry spinning, and hollow spheres were obtained by spray drying. After this pioneering work, the evaporation method has been widely used to fabricate nanomaterials. Li and co-workers synthesized CdO nanotubes with a diameter of 50 nm by using the evaporation of Cd powders without catalysts or templates.<sup>[18]</sup> More recently, a new mesoporous structure (i.e., packed hollow spheres) in silica nanowires has been obtained for the first time by using an evaporation method. This unique structure was formed by the co-assembly of a triblock copolymer (P123) and a silica source, tetraethylorthosilicate (TEOS), in anodized aluminum oxide (AAO) with a channel diameter of 13–200 nm.<sup>[20]</sup> Though the evaporation method has provided a new vision to synthesize nanostructures, some drawbacks of the method prevent its widespread application in the synthesis of hollow materials, for instance, the difficulty in controlling the resulting morphologies and the lack of a good mechanistic understanding of the process.

The templates for the synthesis of hollow materials include hard templates,<sup>[21]</sup> soft templates, such as emulsions<sup>[22]</sup> or micelles,<sup>[23]</sup> and reactive templates based on the Kirkendall effect<sup>[1]</sup> or Ostwald ripening.<sup>[24]</sup> Among these templates, emulsion systems are the most efficient and widely used methods to produce hollow mesoporous silica materials. They may be prepared from oil-in-water,<sup>[22a]</sup>

[a] Key Laboratory of Colloid and Interface Chemistry, Shandong University, Ministry of Education, Jinan, Shandong, 250100, People's Republic of China  
Fax: +86-531-88564750  
E-mail: lqzheng@sdu.edu.cn

water-in-oil,<sup>[22b]</sup> water-oil-water,<sup>[22c]</sup> and oil-water-oil<sup>[22d]</sup> emulsion mixtures. However, emulsion systems do have intrinsic disadvantages, which include low structural robustness, low productive fields, and somewhat complicated synthetic procedures. Therefore, it is still challenging to devise simple methods to synthesize hollow silica materials by using emulsion templates.

Ionic liquids (ILs) are unique organic salts with low melting points, sometimes as low as  $-96\text{ }^{\circ}\text{C}$ .<sup>[25]</sup> In recent years, ILs have received more attention due to their distinctive properties of low melting temperature, nonflammability, high ionic conductivity, negligible vapor pressure, wide electrochemical window, good catalytic properties, and so on.<sup>[26]</sup> One of the most attractive aspects of ILs is that their structure can be conveniently designed to include various physical characteristics. Thus, surface-active ILs have been designed and widely used to direct the synthesis of micro- and nanomaterials in recent years.<sup>[27]</sup> The most extensively investigated ILs are the 1-alkyl-3-methylimidazolium halides ( $\text{C}_n\text{mimX}$ ), where “ $n$ ” indicates the carbon number of the alkyl portion and “X” may be  $\text{Br}^-$  or  $\text{Cl}^-$ . These long-chain ILs display self-organized structures, such as micelles, liquid crystals, vesicles, and emulsions,<sup>[28]</sup> which may be used as templates for the synthesis of nanomaterials.

Although the template-free evaporation and emulsion template synthesis of hollow materials have been developed very quickly in recent years, the combination of these two methods has been rarely reported.<sup>[29]</sup> Mann et al. have successfully synthesized elaborate sponge-like crystalline calcium carbonate materials by a combination of an evaporation method and water-in-oil microemulsion templates.<sup>[29a]</sup> In this work, we describe the combination of evaporation and emulsion templating to synthesize hollow silica materials with the aid of an IL, 1-dodecyl-3-methylimidazolium bromide ( $\text{C}_{12}\text{mimBr}$ ). The materials are also evaluated as controlled release vehicles by using Rhodamine B.

## 2. Results and Discussion

### 2.1. Controlled Synthesis and Characterization of Hollow Silica Spheres and Worm-Like Materials

In this study, the selective synthesis of hollow spheres and worm-like materials is presented. The key factors involve the stirring time and evaporation temperature before pouring the precursor mixture onto a glass substrate. In a typical procedure, a mixture of IL, ammonium hydroxide, and water are added to ethanol at room temperature and stirred for 15 min. A silica precursor (TEOS in the present study) is slowly added to the mixture and stirred for a further time before the entire mixture is poured onto a glass substrate for evaporation and calcination. Thus, microporous hollow microspheres and worm-like materials can easily be synthesized with some modifications in the procedure.

#### 2.1.1. Controlled Synthesis of Hollow Silica Microspheres

When a stirring time before evaporation of five minutes and an evaporation temperature of  $120\text{ }^{\circ}\text{C}$  are employed,

microporous hollow silica microspheres are obtained after calcination. Figure 1 shows the SEM and TEM images of the hollow silica microspheres synthesized under these conditions. As illustrated in Figure 1a, well-defined silica microspheres coexist with a few silica nanoparticles and aggregated blocks in typical samples. The average diameter of these silica microspheres is about  $1\text{--}2\text{ }\mu\text{m}$ . The inner structure is revealed by broken microspheres as shown in Figure 1a and c, and it can be seen that the microspheres possess a hollow structure.

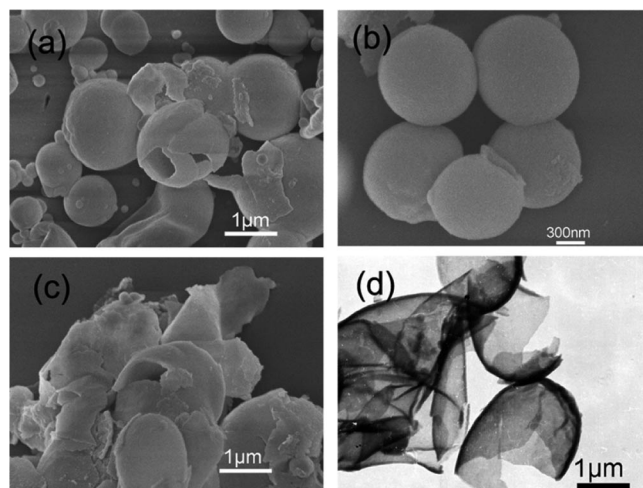


Figure 1. SEM images (a–c) and TEM image (d) of hollow silica microspheres obtained after stirring for five minutes.

To investigate the shell thickness of the hollow silica microspheres, a broken microsphere was measured under high-magnification SEM (Figure 1c). As indicated in the image, the shell thickness is approximately  $75\text{ nm}$ . The TEM image shown in Figure 1d also confirms the hollow structure of the silica materials. The broken fragments of microspheres have an approximate shell thickness of  $70\text{ nm}$ , which is consistent with the results of the SEM measurements.

#### 2.1.2. Controlled Synthesis of Hollow Worm-Like Silica Materials

Alternatively, when the stirring time after TEOS addition is prolonged to 10 min, a silica product with an entirely different morphology is obtained; Figure 2 shows the SEM and TEM images of these products. As illustrated in Figure 2a, the low-magnification SEM image suggests that the resultant products are mostly worm-like in their morphology with a width of about  $1\text{--}2\text{ }\mu\text{m}$ , while their length is not uniform. Some of the worm-like materials exhibit small openings on their surface, also indicating the hollow structure of the silica products, as seen in the high-magnification SEM images (Figure 2b and c). An enlarged image of a hole in the side of a tube (inset, Figure 2b) reveals the hollow interior of the silica worm-like materials. A broken opening at the terminus of one structure was also found (Figure 2c). The average shell thickness is approximately  $70\text{--}80\text{ nm}$ ,

which is similar to the shell thickness of the hollow microspheres described above. TEM was also used to characterize the worm-like materials; the TEM image is shown in Figure 2d. The hollow structure and worm-like morphology are clearly observed. They agree well with SEM images and are analogous to the spheres observed with the shorter stirring time.

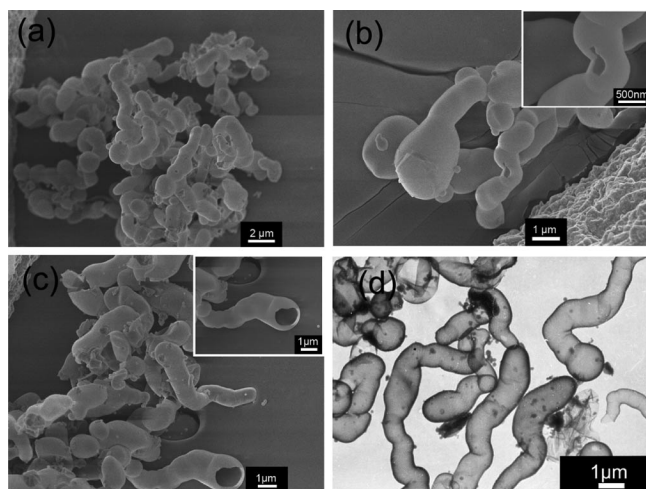


Figure 2. SEM images (a–c) and TEM image (d) of hollow worm-like materials obtained after stirring for ten minutes.

### 2.1.3. Effect of the Temperature

Because the synthesis of these hollow silica materials involves evaporation, the effect of temperature on the observed silica materials was investigated. Figure 3a shows the TEM image of the products obtained at 40 °C after a stirring time of 10 min. It is clear that the products are mostly hollow microspheres. The average diameter of these hollow microspheres is in the range 1–3 μm, with a shell thickness of about 70–100 nm. Regardless of whether the reaction time is 5 or 10 min, the products obtained at 40 °C are mostly hollow microspheres, coexisting with a few irregular structures.

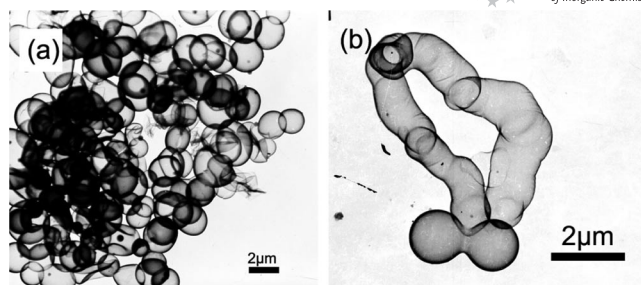


Figure 3. TEM images of silica products obtained at 40 °C (a) and 60 °C (b).

When the temperature is increased to 60 °C, with a stirring time of 10 min (Figure 3b), it can be seen that the products obtained are hollow microspheres mixed with worm-like materials. The image also indicates that these two microspheres are fused together, which is helpful to the better understanding of the formation mechanism. The diameter of the microspheres and structures of the worm-like materials obtained at 60 °C are similar to those of materials obtained at 120 °C. Thus, the evaporation temperature may be modified to change the final morphology of the silica products.

### 2.2. Thermogravimetric Analysis of the Precursors

Thermogravimetric analysis (TGA) curves, measured under a nitrogen atmosphere, of the silica precursors after evaporation and during the calcination process are shown in Figure 4. It is clear that the silica precursor undergoes three steps during calcination with a total weight loss of approximately 54.0%. The first step from 20 to 200 °C resulting in about a 3% weight loss is attributed to the desorption of water and ethanol adsorbed on the silica material. The second, most significant weight loss from 200 to 330 °C of about 36% is assigned to the decomposition of C<sub>12</sub>mimBr attached to the silica material, which is confirmed by comparison to the thermogravimetric analysis curve of C<sub>12</sub>mimBr alone, shown in Figure 4b. From 330 to 600 °C, a final weight loss of about 15% is assigned to the removal of water molecules from the hydroxy groups on the

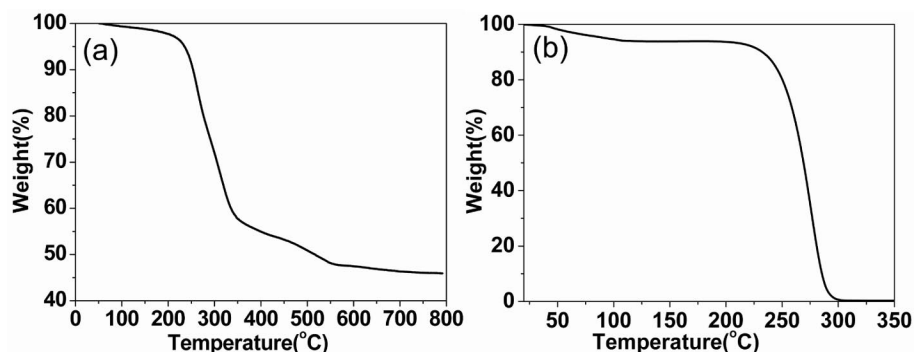


Figure 4. TG analysis of silica precursors (a) and C<sub>12</sub>mimBr (b).



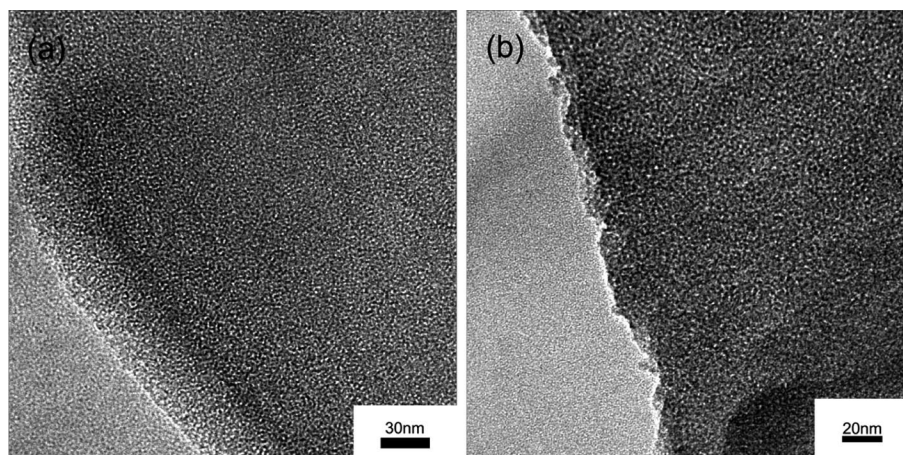


Figure 5. HRTEM images of hollow silica microspheres (a) and worm-like materials (b).

silica and a small amount of residual organic material.<sup>[30]</sup> Above 600 °C, there is no further weight loss, which indicates that the organic component has been removed completely. After calcination, the silica products are generally free of impurities. TGA also indicates that there is a large amount of C<sub>12</sub>mimBr doping of the silica precursors, revealing that the silica materials obtained are formed on the basis of an emulsion template.

### 2.3. HRTEM Characterization of Silica Materials

For further information on the two types of silica samples, HRTEM was used to investigate their structures. Figure 5a shows the HRTEM image of partial silica microspheres. It is clear that there are a large number of nanopores on their surface in the order of 1–5 nm.<sup>[31]</sup> Similarly, the HRTEM image of a worm-like structure is shown in Figure 5b, which also indicates the presence of nanopores.

### 2.4. Brunauer–Emmett–Teller (BET) Analysis

Nitrogen adsorption/desorption is a useful method to characterize porous solids, to evaluate the specific surface area, pore size, pore-size distribution, and pore volume of a material.<sup>[32]</sup> Brunauer–Emmett–Teller (BET) analyses were

performed to determine the surface areas and pore sizes of the corresponding hollow silica microspheres and worm-like materials. The typical nitrogen adsorption/desorption isotherms of hollow microspheres are illustrated in Figure 6a. The observed curve is attributed to a predominantly microporous structure. The surface area ( $S_{\text{BET}}$ ) calculated by using the BET equation is about 537 m<sup>2</sup> g<sup>−1</sup>, and the pore volume is about 0.343 cm<sup>3</sup> g<sup>−1</sup>. The pore-size distribution (inset, Figure 6a) ranges from 1 to 2.5 nm with a mean size of 1.41 nm. Figure 6b shows the typical nitrogen adsorption/desorption isotherms of the hollow worm-like materials. The BET surface area and the total pore volume are 271 m<sup>2</sup> g<sup>−1</sup> and 0.211 cm<sup>3</sup> g<sup>−1</sup>, respectively. The pore-size distribution determined from the adsorption branch shows a sharp peak at 1.45 nm together with two small peaks located at 2.69 nm and 4.21 nm, and the average pore size is about 1.48 nm. In comparison, the hollow microspheres have a larger surface area and smaller pore size than the worm-like materials, because the hollow silica microspheres have a relatively smaller pore diameter.

### 2.5. Formation Mechanism

In order to explore the role of C<sub>12</sub>mimBr in the synthesis process, a control experiment was performed. A similar syn-

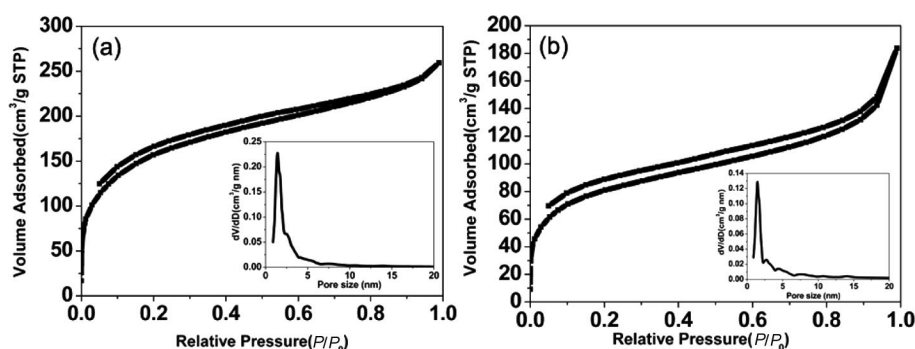


Figure 6. N<sub>2</sub> adsorption/desorption isotherms of hollow silica microspheres (a) and hollow worm-like materials (b). The insets indicate the pore-size distribution determined from the absorption branch.

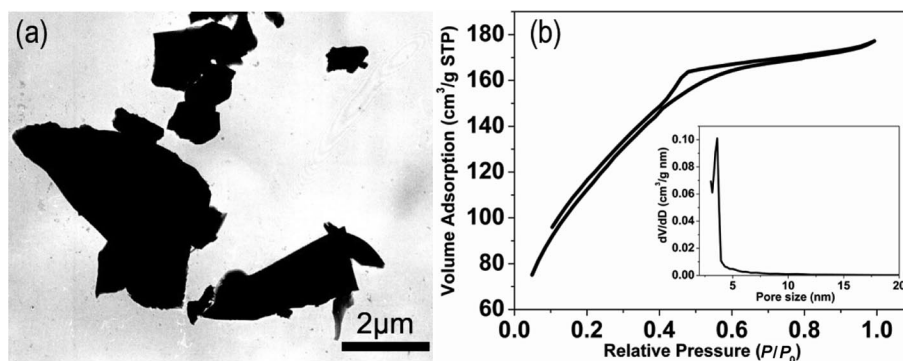


Figure 7. TEM image (a) and  $N_2$  adsorption/desorption isotherm (b) of silica products synthesized without  $C_{12}mimBr$ . The inset indicates the pore-size distribution determined from the adsorption branch.

thetic procedure was carried out to prepare the silica materials in the absence of  $C_{12}mimBr$ . From the TEM image of the resultant products under these conditions (Figure 7a), no structured materials were found except the irregular aggregated blocks. This highlights the role  $C_{12}mimBr$  has played as an emulsion template in the synthesis procedure. Figure 7b shows the typical nitrogen adsorption/desorption isotherms of irregular silica blocks. The BET surface area and pore size are  $418 \text{ m}^2 \text{ g}^{-1}$  and 3.61 nm, respectively. Although the surface area of the irregular aggregated blocks is comparable to that of hollow silica microspheres and worm-like materials, their formation mechanisms are distinct. The pores formed without  $C_{12}mimBr$  are due to the aggregation of silica nanoparticles, which results in the appearance of the pores between the space intervals of the aggregated nanoparticles.<sup>[33]</sup>

A model based on the above experimental results for the formation of the hollow microspheres and hollow worm-like materials is sketched out in Figure 8. An oil (TEOS)-in-water (aqueous solution) emulsion is generated by adding TEOS to the mixture of water and ethanol in the presence of  $C_{12}mimBr$ . The TEOS oil cores are surrounded by  $C_{12}mimBr$  which is absorbed at the interface of the TEOS and water. Throughout the alkali catalysis, TEOS molecules are hydrolyzed and condense along the interface.<sup>[34]</sup> When the stirring time is relatively short (5 min), hollow microspheres that keep the spherical morphology of the emulsion template are formed. When the stirring time is prolonged to 10 min, some spherical droplets start to fuse as a result of their dynamic instability.<sup>[35]</sup> Some fused microspheres may be formed at this stage, as illustrated in Figure 3b. The fused microspheres may further grow through additional fusion of spheres, resulting in the final worm-like silica materials. At low temperature ( $40^\circ\text{C}$ ), the movement of emulsion droplets is relatively slower, and only microspheres are observed; the fusing of the microspheres is not favored. However, a relatively high temperature causes the emulsion droplets to move faster, which accelerates the process of fusion. As a result, the worm-like silica material dominates at the higher temperatures. Finally, evaporation plays a significant role in the formation of the micropores in the hollow microspheres and worm-like materials. In the synthesis pro-

cedure, the evaporation process is employed to increase the evaporation rate of the volatile components (e.g. water and ethanol) from the emulsified precursor solution. This evaporation procedure is the driving force for generating a well-ordered lyotropic liquid crystalline (LLC) phase within the droplets.<sup>[36]</sup> This would provide proper conditions to cause the appearance of well-ordered microporous structures.

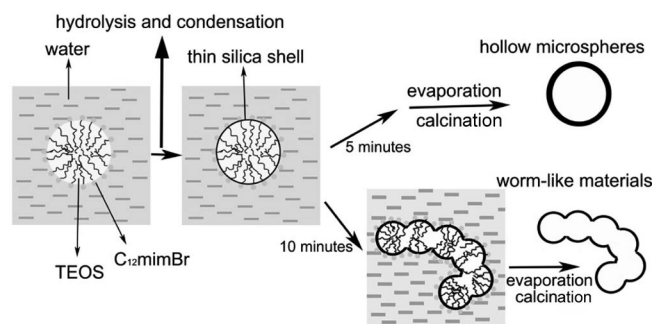


Figure 8. Schematic illustration of the morphology-controlled synthesis of hollow silica microspheres and worm-like materials.

## 2.6. In Vitro Controlled Release

Typical controlled release profiles for the two different types of silica material synthesized here are plotted in Figure 9a and b. Both studies were performed under the same conditions. There is no substantial difference in the release profiles of hollow silica microspheres or worm-like materials. A release percentage of 50% is detected after about 60 min and a percentage of 90% after about 360 min for the hollow microspheres, while a 50% and 90% release for the worm-like hollow materials is detected after 70 and 360 min, respectively. In the initial release stage, there is burst release behavior for both silica materials. This initial behavior is attributed to two reasons:<sup>[8]</sup> First, there is excess Rhodamine B weakly entrapped in the micropores or located on the outer surface of the silica materials, which is easily released. Second, the burst release from the hollow silica materials at the beginning is caused by the concentration gradient between the cores of the materials and the

surrounding aqueous solution. After the burst release, the Rhodamine B is found to be released slowly from the hollow silica materials. These two-step release profiles can be fitted to a hyperbolic function:<sup>[37]</sup>

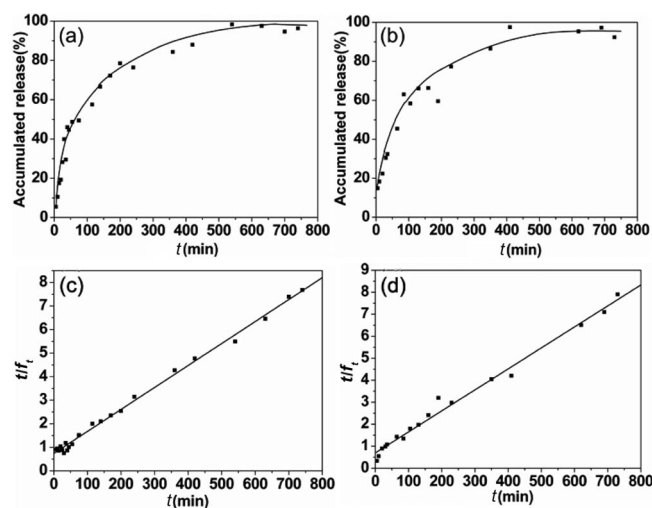


Figure 9. Controlled release of Rhodamine B from hollow silica microspheres (a) and hollow worm-like materials (b). Linearized functions of hollow silica microspheres (c) and hollow worm-like materials (d).

$$f_t = t/(a + bt)$$

where  $a$  and  $b$  are adjustable parameters:  $1/a$  is the initial release rate,  $1/b$  is the maximum release fraction, and  $f_t$  is the fraction of Rhodamine B release at time  $t$ . This function can be transformed to

$$t/f_t = a + bt$$

where the parameters  $a$  and  $b$  can be obtained from the experimental results. Figure 9c and d show the plot of  $(t/f_t)$  as a function of  $t$  for the hollow microspheres and worm-like materials. By analyzing the profiles, the maximum release fraction ( $1/b$ ) and the initial release rate ( $1/a$ ) can be obtained and is shown in Table 1, in which  $R$  is the correlation coefficient. The final maximum release fractions from the profiles are more than 100%, which may be attributed to the experimental error of the measurement. The hollow worm-like materials have a higher initial release rate, but both materials display suitable controlled release ability. Thus, the hollow microspheres and worm-like structures have potential applications in the drug release field.

Table 1. Kinetic parameters of Rhodamine B release for silica microspheres and hollow worm-like materials.

	Maximum release fraction	Initial release rate	$R$
Hollow microspheres	107	1.35	0.998
Worm-like materials	105	1.44	0.994

### 3. Conclusion

In summary, we have demonstrated a novel and facile method to synthesize hollow silica microspheres and hollow

worm-like silica materials through the combination of an evaporation method with the use of an emulsion template. The morphology of silica materials that can be selectively synthesized ranges from hollow microspheres to worm-like materials by using an IL,  $C_{12}mimBr$ , and by adjusting the stirring time and temperature of the IL/silica precursor mixture. A plausible mechanism is put forward to explain the formation of hollow microspheres and worm-like materials. The materials were both characterized by nitrogen adsorption/desorption analysis, which indicates a large surface area and the existence of micropores on the surface of the samples. Due to the microporous structures of the two samples, both materials show suitable ability as controlled release systems in vitro. The combination of evaporation and the use of an emulsion template represents a new pathway in the preparation of hollow silica materials. On the basis of this technique, other micro- or macroporous materials with hollow structure may also be expected to be prepared.

## 4. Experimental Section

**4.1. Samples:**  $C_{12}mimBr$  was prepared according to the procedure reported by Dupont et al.<sup>[38]</sup> Analytical grade ammonium hydroxide  $NH_3 \cdot H_2O$  (25 to 28%) was purchased from Laiyang Chemical Reagents Co. Ltd. China, and ethanol ( $\geq 99.7\%$ ) from Tianjin Damao Chemical Reagents Co. Ltd. China. The silica source tetraethyloxysilicate (TEOS,  $\geq 98\%$ ), was purchased from Beijing Yili Chemical Reagents Co. Ltd. China, and Rhodamine B from Salland-chem International Inc.; all reagents were used as received. Doubly distilled water was used in all experiments.

### 4.2. Preparation

**4.2.1. Synthesis of Hollow Microspheres and Worm-Like Materials:** In a typical synthesis, a  $C_{12}mimBr$  solution (0.5 mL, 0.054 M), water (0.8 mL), and ammonia solution (0.5 mL, 1.25 wt%) were mixed with ethanol (2.0 mL) at 25 °C. After stirring for 15 min, TEOS (0.15 mL) was slowly added to the solution. After additional stirring for 5 or 10 min, the mixture was poured onto a glass substrate and placed into an oven at 120 °C, in which it was kept for 4 h. Finally, the resulting white precipitates were calcined at 600 °C for 6 h, cooled, and examined. When the stirring time was 5 min, hollow microspheres were obtained; after a stirring time of 10 min, worm-like structures were obtained. Figure 10 shows a flowchart of the synthesis of silica products by the evaporation method.

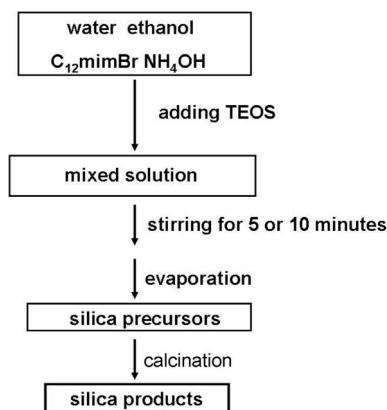


Figure 10. Synthesis of silica products by the evaporation method.



**4.2.2. Synthesis of Controlled Release Vehicles:** To load the hollow materials with Rhodamine B, hollow microspheres or worm-like materials (5 mg) were placed in a vial containing Rhodamine B (1 mg) in water (1 mL). The mixture was stirred for 48 h. It was then centrifuged and washed with deionized water three times. Finally, the products were dried in a vacuum oven at 40 °C for 6 h. For the controlled release experiment, the silica material loaded with Rhodamine B was dispersed in water (100 mL) and stirred at room temperature. At predetermined time intervals, an aliquot (0.5 mL) was taken from the release medium and centrifuged, and the filtrates were diluted to 2.0 mL. The amount of Rhodamine B released from the samples was determined by UV/Vis spectrophotometry at an analytical wavelength of 554 nm.<sup>[39]</sup> Release experiments were conducted until the concentration of the solution stopped changing significantly.

**4.3. Characterization:** The sizes and morphologies of the synthesized silica materials were characterized by transmission electron microscopy (JEOL JEM-100CXII). The samples were made by placing a drop of the silica materials diluted in ethanol onto carbon-coated copper grids. After evaporation of the excess solvent, the particles were observed at an operating voltage of 80 kV. Scanning electron microscopy with a JEOL JSM-7600F instrument operating at 3.0 kV was also performed to measure the sizes and morphologies of silica materials. The method of fabricating samples for SEM was almost the same as that for TEM, except that the samples were sputtered with gold before detection in order to enhance their electrical conductivity. High-resolution transmission electron microscopy (JEOL JEM-2100) was also employed to characterize the morphologies and microstructures with an accelerating voltage of 200 kV. Thermal gravimetric analysis (TGA) was carried out with a SDTQ600 thermal analyzer (TA Instruments, Ltd.) under N<sub>2</sub> over a temperature range of 25 to 800 °C with a heating rate of 10 °C/min. The concentration of Rhodamine B was monitored in a 1.0 cm quartz cell with a UV/Vis spectrophotometer (HP 8453E) at 554 nm. Nitrogen adsorption/desorption measurements were performed with a QuadraSorb SI apparatus. The surface areas of the materials were calculated by using the Brunauer–Emmett–Teller (BET) method, and the pore-size distribution was calculated from the adsorption isotherms by using the Brunauer–Joyner–Halenda (BJH) method.

## Acknowledgments

The work was supported by the National Natural Science Foundation of China (No.50972080), the Laboratory of Organic Optoelectronic Functional Materials and Molecular Engineering, the Technical Institute of Physics and Chemistry (TIPC), and the Chinese Academy of Sciences (CAS). The authors thank Dr. J. David Van Horn (Visiting Professor, Shandong University) for editorial assistance.

- [1] Y. D. Yin, R. M. Rioux, C. K. Erdonmez, S. Hughes, G. A. Somorjai, A. P. Alivisatos, *Science* **2004**, *304*, 711–714.
- [2] a) Y. G. Sun, Y. N. Xia, *Science* **2002**, *298*, 2176–2179; b) B. H. Sohn, J. M. Choi, S. Yoo, S. H. Yun, W. C. Zin, J. C. Jung, M. Kanehara, T. Hirata, T. Teranishi, *J. Am. Chem. Soc.* **2003**, *125*, 6368–6369; c) M. W. Zhao, N. Li, L. Q. Zheng, G. Z. Li, L. Yu, *J. Dispersion Sci. Technol.* **2008**, *29*, 1103–1105; d) M. Q. Zhu, L. Q. Wang, G. J. Exarhos, A. D. Q. Li, *J. Am. Chem. Soc.* **2004**, *126*, 2656–2657.
- [3] a) B. H. Hong, S. C. Bae, C. W. Lee, S. Jeong, K. S. Kim, *Science* **2001**, *294*, 348–351; b) K. M. Ryan, D. Ertz, H. Olin, M. A. Morris, J. D. Holmes, *J. Am. Chem. Soc.* **2003**, *125*, 6284–6288; c) L. Cademartiri, G. A. Ozin, *Adv. Mater.* **2009**, *21*, 1013–1020; d) K. Kang, D. A. Kim, H. S. Lee, C. J. Kim, J. E. Yang, M. H. Jo, *Adv. Mater.* **2008**, *20*, 4684–4690.
- [4] a) S. Iijima, *Nature* **1991**, *354*, 56–58; b) M. D. Lynch, D. L. Patrick, *Nano Lett.* **2002**, *2*, 1197–1201; c) S. M. Yoon, I. C. Hwang, K. S. Kim, H. C. Choi, *Angew. Chem. Int. Ed.* **2009**, *48*, 2506–2509; d) R. Kreizman, S. Y. Hong, J. Sloan, R. Popovitz-Biro, A. Albu-Yaron, G. Tobias, B. Ballesteros, B. G. Davis, M. L. H. Green, R. Tenne, *Angew. Chem. Int. Ed.* **2009**, *48*, 1230–1233.
- [5] a) X. J. Wu, D. S. Xu, *J. Am. Chem. Soc.* **2009**, *131*, 2774–2775; b) W. Z. Wang, Y. J. Zhan, G. H. Wang, *Chem. Commun.* **2001**, *8*, 727–728; c) A. Narayanaswamy, H. F. Xu, N. Pradhan, M. Kim, X. G. Peng, *J. Am. Chem. Soc.* **2006**, *128*, 10310–10319; d) J. Y. Chen, B. Wiley, Z. Y. Li, D. Campbell, F. Saeki, H. Cang, L. Au, J. Lee, X. D. Li, Y. N. Xia, *Adv. Mater.* **2005**, *17*, 2255–2261.
- [6] B. Lim, M. J. Jiang, J. Tao, P. H. C. Camargo, Y. M. Zhu, Y. N. Xia, *Adv. Funct. Mater.* **2008**, *18*, 1–12.
- [7] H. T. Shi, L. M. Qi, J. M. Ma, H. M. Cheng, *J. Am. Chem. Soc.* **2003**, *125*, 3450–3451.
- [8] a) S. W. Song, K. Hidajat, S. Kawi, *Langmuir* **2005**, *21*, 9568–9575; b) S. S. Huang, Y. Fan, Z. Y. Cheng, D. Y. Kong, P. P. Yang, Z. W. Quan, C. M. Zhang, J. Lin, *J. Phys. Chem. C* **2009**, *113*, 1775–1784; c) J. Yang, J. Lee, J. Kang, K. Lee, J. S. Suh, H. G. Yoon, Y. M. Huh, S. Haam, *Langmuir* **2008**, *24*, 3417–3421.
- [9] a) J. B. Fei, Y. Cui, X. H. Yan, W. Qi, Y. Yang, K. W. Kang, Q. He, J. B. Li, *Adv. Mater.* **2008**, *20*, 452–456; b) S. W. Kim, M. Kim, W. Y. Lee, T. Hyeon, *J. Am. Chem. Soc.* **2002**, *124*, 7642–7643.
- [10] a) J. Y. Chen, D. L. Wang, J. F. Xi, L. Au, A. Siekkinen, A. Warsen, Z. Y. Li, H. Zhang, Y. N. Xia, X. D. Li, *Nano Lett.* **2007**, *7*, 1318–1322; b) Y. G. Sun, Y. N. Xia, *Anal. Chem.* **2002**, *74*, 5297–5305.
- [11] Z. L. Wang, J. H. Song, *Science* **2006**, *312*, 242–246.
- [12] a) C. J. Martinez, B. Hocky, C. B. Montgomery, S. Semancik, *Langmuir* **2005**, *21*, 7937–7944; b) J. Y. Chen, F. Saeki, B. J. Wiley, H. Cang, M. J. Cobb, Z. Y. Li, L. Au, H. Zhang, M. B. Kimmey, X. D. Li, Y. N. Xia, *Nano Lett.* **2005**, *5*, 473–477; c) H. Cang, T. Sun, Z. Y. Li, J. Y. Chen, B. J. Wiley, Y. N. Xia, X. D. Li, *Opt. Lett.* **2005**, *30*, 3048–3050.
- [13] M. Iida, T. Sasaki, M. Watanabe, *Chem. Mater.* **1998**, *10*, 3780–3782.
- [14] Y. F. Lu, H. Y. Fan, A. Stump, T. L. Ward, T. Rieker, C. J. Brinker, *Nature* **1999**, *398*, 223–226.
- [15] J. J. Zhu, S. Xu, H. Wang, J. M. Zhu, H. Y. Chen, *Adv. Mater.* **2003**, *15*, 156–159.
- [16] A. M. Herring, J. T. McKinnon, B. D. McCloskey, J. Filley, K. W. Gneshin, R. A. Pavelka, H. J. Kleebe, D. J. Aldrich, *J. Am. Chem. Soc.* **2003**, *125*, 9916–9917.
- [17] P. J. Bruinsma, A. Y. Kim, J. Liu, S. Baskaran, *Chem. Mater.* **1997**, *9*, 2507–2512.
- [18] H. B. Lu, L. Liao, H. Li, Y. Tian, D. F. Wang, J. C. Li, Q. Fu, B. P. Zhu, Y. Wu, *Mater. Lett.* **2008**, *62*, 3928–3930.
- [19] G. M. Li, X. C. Wang, Y. H. Wang, X. W. Shi, N. Yao, B. L. Zhang, *Physica E* **2008**, *40*, 2649–2653.
- [20] P. Lai, M. Z. Hu, D. L. Shi, D. Blom, *Chem. Commun.* **2008**, 1338–1340.
- [21] a) F. Caruso, R. A. Caruso, H. Möhwald, *Science* **1998**, *282*, 1111–1114; b) F. Caruso, X. Y. Shi, R. A. Caruso, A. Susha, *Adv. Mater.* **2001**, *13*, 740–744; c) M. L. Breen, A. D. Dinsmore, R. H. Pink, S. B. Qadri, B. R. Ratna, *Langmuir* **2001**, *17*, 903–907; d) Z. F. Dai, L. Dähne, H. Möhwald, B. Tiersch, *Angew. Chem. Int. Ed.* **2002**, *41*, 4019–4022.
- [22] a) C. I. Zoldesi, A. Imhof, *Adv. Mater.* **2005**, *17*, 924–928; b) W. J. Li, X. X. Sha, W. J. Dong, Z. C. Wang, *Chem. Commun.* **2002**, 2434–2435; c) M. Fujiwara, K. Shiokawa, Y. Tanaka, Y. Nakahara, *Chem. Mater.* **2004**, *16*, 5420–5426; d) W. J. Li, M. C. Coppins, *Chem. Mater.* **2005**, *17*, 2241–2246; e) M. W.

- Zhao, L. Q. Zheng, N. Li, L. Yu, *Mater. Lett.* **2008**, *62*, 4591–4593.
- [23] a) T. B. Liu, Y. Xie, B. Chu, *Langmuir* **2000**, *16*, 9015–9022; b) J. L. Blin, A. Léonard, Z. Y. Yuan, L. Gigot, A. Vantomme, A. K. Cheetham, B.-L. Su, *Angew. Chem. Int. Ed.* **2003**, *42*, 2872–2875; c) D. B. Zhang, L. M. Qi, J. M. Ma, H. M. Cheng, *Adv. Mater.* **2002**, *14*, 1499–1502.
- [24] a) H. G. Yang, H. C. Zeng, *J. Phys. Chem. B* **2004**, *108*, 3492–3495; b) W. S. Wang, L. Zhen, C. Y. Xu, L. Yang, W. Z. Shao, *J. Phys. Chem. C* **2008**, *112*, 19390–19398; c) R. Qiao, X. L. Zhang, R. Qiu, J. C. Kim, Y. S. Kang, *Chem. Mater.* **2007**, *19*, 6485–6491; d) P. Hu, L. J. Yu, A. H. Zuo, C. Y. Guo, F. L. Yuan, *J. Phys. Chem. C* **2009**, *113*, 900–906.
- [25] T. L. Greaves, C. J. Drummond, *Chem. Rev.* **2008**, *108*, 206–237.
- [26] a) M. Paliakoff, J. M. Fitzpatrick, T. R. Farren, P. T. Anastas, *Science* **2002**, *297*, 807–810; b) S. G. Kazarian, B. J. Briscoe, T. Welton, *Chem. Commun.* **2000**, 2047–2048; c) R. D. Rogers, K. R. Seddon, *Science* **2003**, *302*, 792–793.
- [27] a) D. B. Kuang, T. Brezesinski, B. Smarsly, *J. Am. Chem. Soc.* **2004**, *126*, 10534–10535; b) B. G. Trewyn, C. M. Whitman, V. S. Y. Lin, *Nano Lett.* **2004**, *4*, 2139–2143; c) Y. Zhou, M. Antonietti, *Chem. Mater.* **2004**, *16*, 544–550.
- [28] a) G. A. Baker, S. Pandey, S. Pandey, S. N. Baker, *Analyst* **2004**, *129*, 890–892; b) C. J. Bowles, D. W. Bruce, K. R. Seddon, *Chem. Commun.* **1996**, 1625–1626; c) J. C. Hao, A. X. Song, J. Z. Wang, X. Chen, W. C. Zhuang, F. Shi, F. Zhou, W. M. Liu, *Chem. Eur. J.* **2005**, *11*, 3936–3940; d) Y. A. Gao, J. Zhang, H. Y. Xu, X. Y. Zhao, L. Q. Zheng, X. W. Li, L. Yu, *ChemPhysChem* **2006**, *7*, 1554–1561.
- [29] a) D. Walsh, B. Lebeau, S. Mann, *Adv. Mater.* **1999**, *11*, 324–328; b) O. J. Carye, S. Biggs, *J. Mater. Chem.* **2009**, *19*, 2724–2728.
- [30] Q. F. Lu, D. R. Chen, X. L. Jiao, *Chem. Mater.* **2005**, *17*, 4168–4173.
- [31] Y. Zhou, J. H. Schattka, M. Antonietti, *Nano Lett.* **2004**, *4*, 477–481.
- [32] a) M. Kruk, M. Jaroniec, A. Sayari, *J. Phys. Chem. B* **1997**, *101*, 583–589; b) M. Jaroniec, M. Kruk, J. P. Olivier, *Langmuir* **1999**, *15*, 5410–5413.
- [33] a) B. E. Yoldas, M. J. Annen, J. Bostaph, *Chem. Mater.* **2000**, *12*, 2475–2484; b) C. Alié, A. Benhaddou, R. Pirard, A. J. Lecloux, J. P. Pirard, *J. Non-Cryst. Solids* **2000**, *270*, 77–90.
- [34] Y. S. Li, J. L. Shi, Z. L. Hua, H. R. Chen, M. L. Ruan, D. S. Yan, *Nano Lett.* **2003**, *3*, 609–612.
- [35] C. Tao, J. B. Li, *Colloids Surf. A* **2005**, *256*, 57–60.
- [36] a) C. J. Brinker, Y. F. Lu, A. Sellinger, H. Y. Fan, *Adv. Mater.* **1999**, *11*, 579–585; b) C. F. Xue, B. Tu, D. Y. Zhao, *Adv. Funct. Mater.* **2008**, *18*, 3914–3921; c) N. Andersson, B. Kronberg, R. Corkery, P. Alberius, *Langmuir* **2007**, *23*, 1459–1464.
- [37] D. Acros, A. López-Noriega, E. Ruiz-Hernández, O. Terasaki, M. Vallet-Regí, *Chem. Mater.* **2009**, *21*, 1000–1009.
- [38] J. Dupont, C. S. Consorti, P. A. Z. Suarez, R. F. de Souza, *Org. Synth.* **2002**, *79*, 236–240.
- [39] S. K. Das, J. Bhowal, A. R. Das, A. K. Guha, *Langmuir* **2006**, *22*, 7265–7272.

Received: July 28, 2009

Published Online: January 12, 2010